Truncated Weighted Nuclear Norm Regularization and Sparsity for Image Denoising

MingYan Zhang[1], Mingli Zhang[2], Feng Zhao[1], Fan Zhang[1] and Alan Evans[2]
1. School of Computer Science, Shandong Technology and Business University, China
2. Montreal Neurological Institute, McGill University
Correspondence: Mingli.Zhang@mcgill.ca

ABSTRACT

The attribute of signal sparsity is widely used to sparse representation. The existing nuclear norm minimization and weighted nuclear norm minimization may achieve a suboptimal in real application with the inaccurate approximation of a rank function. This paper presents a novel denoising method that preserves fine structures in the image by imposing $L1$ norm constraints on the wavelet transform coefficients and low rank on high-frequency components of group similar patches. An efficient proximal operator of Truncated Weighted Nuclear Norm (TWNN) is proposed to accurately recover the underlying high-frequency components of low-rank patches. By combining a wavelet domain sparse preservation prior with TWNN, the proposed method significantly improves the reconstruction accuracy, leading to a higher PSNR/SSIM and visual quality than the state of the art approaches.

Introduction

Image denoising is an important pre-processing step that has a broad range of applications in computer vision and graphics. Formally, image denoising can be defined as the task of recovering the original image $\boldsymbol{x}$ from its underlying noisy observation $\boldsymbol{y} = \boldsymbol{x} + \boldsymbol{v}$, where $\boldsymbol{v}$ represents additive noise typically assumed to be zero mean Gaussian with standard deviation σ. Most denoising methods exploit the fact that small patches of pixels in an image are similar to other, possibly distant patches of the same image. Approaches using this principle, known as non-local self-similarity(NSS), have obtained state of the art results on many denoising tasks. Moreover, it has been shown that matrices of non-local similar patches have a low rank, and that exploiting this concept can improve the reconstruction of images. In this work, we propose to apply low rank on the high-frequency components of the matrices of non-local similar patches. Nuclear norm minimization (NNM) is the well known convex surrogate function, which aims at finding the lowest rank approximation X of an observed matrix Y:

$$\underset{X}{\operatorname{argmin}} \ \frac{1}{2}\|Y - X\|_F^2 + \lambda\|X\|_*, \tag{1}$$

where $\|X\|_* = \sum_j \sigma_j(X)$ is the nuclear (or trace) norm of X, corresponding to the sum of its singular values $\sigma_j(X)$. The nuclear norm of a matrix is known as the widely used convex approximation of its rank. The truncated nuclear norm regularization (TNNR) method well approximates the rank of matrix with truncated nuclear norm, but ignores that each singular value should be shrunk adaptively. In this paper, we proposed a novel Truncated Weighted Nuclear Norm Minimization. In this paper, we propose a novel and high-performance denoising method by imposing l_1 norm sparsity constraints on wavelet domain and effective truncated weighted nuclear norm (TWNN) minimization stratege on the high-frequency components of matrices stacked by non-local similar patches. The main contributions of this work are as follows:

1 A novel method is proposed, which combines denoising prior based on the wavelet domain l_1 norm sparse prior with non-local truncated weighted nuclear norm (TWNN) minimization on high−frequncy components. Allowing the method to preserve image details corresponding to fine structures and textures.
2 A new proximal operator truncated weighted nuclear norm (TWNN) minimization is proposed to recover the non-local low rank patches in an flexiable and accurate way.
3 The proposed method outperforms state-of-the-art methods in both PSNR SSIM and visual performance on texture images, standard widely used images and real noise images.

Methods

The standard low rank model for non-local patch-based denoising is as follows. Let $\boldsymbol{y} \in \mathbb{R}^N$ be the observed noisy image, and $\boldsymbol{x} \in \mathbb{R}^N$ the denoised image that needs to be recovered from $\boldsymbol{y}$. The main assumption of the model is that the patch of pixels surrounding a pixel in $\boldsymbol{x}$ is similar to other patches in this image, and that the groups of similar patches have a low rank. Let $\boldsymbol{p}_i \in \mathbb{R}^M$ be the patch of M denoised pixels centered on a pixel i, and R_i a pixel selection matrix such that $\boldsymbol{p}_i = R_i\boldsymbol{x}$. Moreover, let $P \in \mathbb{R}^{M\times N}$ be the matrix of patches, i.e. $P = [\boldsymbol{p}_1 \ldots \boldsymbol{p}_N]$. For each pixel i, we define as $Q_i \in \mathbb{R}^{M\times K}$ the matrix containing the K patches most similar to $\boldsymbol{p}_i$. Q_i can be defined as $Q_i = Q_{Hi} + f_L \otimes Q_{Ci}$, where Q_{Hi} is the high-frequency component and Q_{Ci} is the constant component,f_L is low pass filter of size 3×3, $\otimes$ is convolution operator.
The denoising task can then be formulated as the following optimization problem:

$$\begin{aligned} &\underset{\boldsymbol{x}}{\operatorname{argmin}} \ \frac{1}{2\sigma^2}\|\boldsymbol{x} - \boldsymbol{y}\|_2^2 + \lambda\sum_{i=1}^{N}\|Q_{Hi}\|_* \\ &\text{s.t. } \boldsymbol{p}_i = R_i\boldsymbol{x}, Q_i = Q_{Hi} + f_L \otimes Q_{Ci}, \ i = 1\ldots N. \end{aligned} \tag{2}$$

The first term of this formulation minimizes the difference between the denoised image $\boldsymbol{x}$ and the observed image $\boldsymbol{y}$. The second term imposes the group of similar patches Q_i with its high-frequncy component Q_{Hi} to be much low rank, where the rank is approximated using the nuclear norm. This term can be seen as a prior on $\boldsymbol{x}$. Parameter λ controls the trade-off between these two terms.
Let $Y \in \mathbb{R}^{N\times M}$ be an observed data matrix and denote as $\boldsymbol{\omega} \in \mathbb{R}^T$, $T = \min\{M, N\}$, a vector of weights such that $0 = \omega_{j-1} \leq \omega_j \leq \ldots \leq \omega_T$. The truncated weighted nuclear norm proximal problem consists in finding an approximation X of Y, minimizing the following cost function:

$$\underset{X}{\operatorname{argmin}} \ \frac{1}{2}\|Y - X\|_F^2 + \lambda\|X\|_{*,\boldsymbol{\omega}}, \tag{3}$$

where $\|X\|_{*,\boldsymbol{\omega}} = \sum_1^{j-1}\sigma_j(X) + \sum_j^T \omega_j\sigma_j(X)$ is the truncated weighted nuclear norm, which means doing soft-thresholding from the j-th biggest singular value. Based on the experiments, $j = 2$ for image denoising. Denote as $U\Sigma V^\top$ the SVD decomposition of Y, and let $(x)_+ = \max\{x, 0\}$. The optimal solution to this problem is given by the truncated weighted singular value thresholding operator:

$$\mathcal{S}_{\boldsymbol{\omega},\lambda}(Y) = U\Big(\Sigma - \lambda\,\mathrm{Diag}(\boldsymbol{\omega})\Big)_+ V^\top. \tag{4}$$

We use the truncated weighted nuclear norm to impose low rank constraints on the high-frequency components of groups of similar patches Q_{Hi}. We define the thresholding weights as $\omega_j = \alpha\sqrt{K}/(\sigma_j + \varepsilon)$, where $\alpha > 0$ is a user supplied constant and $\varepsilon = 10^{-16}$.
To well preserve the image global structure, we apply l_1 norm sparse on LH and HL subbands of 2D Haar DWT in the first level image decomposition. Denote as $\mathcal{D}_d\boldsymbol{x}$ the image haar DWT operator, where d can be LH or HL subbands. To modeling the Wavelet coefficients more sparsity, the mean coefficients ($\boldsymbol{\mu}_d$) of $\mathcal{D}_d\boldsymbol{x}$ are abstracted. Then the wavelet domain l_1 norm sparse prior can be formulated as:

$$\underset{\mathcal{D}_d\boldsymbol{x}}{\operatorname{argmin}} \sum_{d\in\{LH,HL\}} \|\mathcal{D}_d\boldsymbol{x} - \boldsymbol{\mu}_d\|_1 \tag{5}$$

Considering the proposed truncated weighted nuclear norm on high-frequncy components of matrices with non-local similar patches and wavelet domain l_1 norm sparse prior, the denoising model becomes:

$$\begin{aligned} &\underset{\boldsymbol{x}}{\operatorname{argmin}} \ \frac{1}{2\sigma^2}\|\boldsymbol{x} - \boldsymbol{y}\|_2^2 + \lambda\sum_{i=1}^{N}\|Q_{Hi}\|_{*,\boldsymbol{\omega}} \\ &\qquad + \eta\sum_{d\in\{LH,HL\}}\|\mathcal{D}_d\boldsymbol{x} - \boldsymbol{\mu}_d\|_1 \\ &\text{s.t. } \boldsymbol{p}_i = R_i\boldsymbol{x}, Q_i = Q_{Hi} + f_L \otimes Q_{Ci}, i = 1\ldots N. \end{aligned} \tag{6}$$

The complete optimization process is summarized in Algorithm 1.

Algorithm 1: TWNN and sparsity denoising

Input: The noisy image $\boldsymbol{y}$, $\hat{\boldsymbol{x}}^{(0)} = \boldsymbol{y}$, $\hat{\boldsymbol{y}}^{(0)} = \boldsymbol{y}$;
Input: Parameters λ, μ, η, α and $T_{\max}$;
Output: The denoised image $\boldsymbol{x}$;

Set $\boldsymbol{x} = \boldsymbol{x}_{iter} = \boldsymbol{y}$;

for $t = 1, \ldots, T_{\max}$ **do**
- Iterative Regularization: $\boldsymbol{y}^{(t)} = \eta\hat{\boldsymbol{x}}^{(t-1)} + \delta(\boldsymbol{y} - \boldsymbol{y}^{(t-1)})$;
- Update noise variance σ^2;
- Update patches: $\boldsymbol{p}_i = R_i\boldsymbol{x}$, $i = 1, \ldots, N$;
- Update similar patches groups Q_i, $i = 1, \ldots, N$;
- Update low rank patches $\widehat{Q}_i$, $i = 1, \ldots, N$, using Eq. (12);
- Update histogram mapping functions F_d using Eq. (8);
- Reconstruct image $\widehat{\boldsymbol{x}}$ from low rank patches using Eqs. (14) and (15);

return $\boldsymbol{x}$;

Results

Table I: PSNR (dB) and SSIM obtained by the tested methods on the 10 high definition images for various noise levels. Best results for each image are highlighted in bold font.

	σ = 20					
	BM3D	LSSC	NCSR	WNNM	S-GHP	Ours
1	30.83	30.69	30.59	30.81	30.60	**30.91**
	0.876	0.872	0.869	0.873	0.869	**0.879**
2	28.07	27.98	27.91	27.96	27.97	**28.14**
	0.817	0.815	0.807	0.807	0.814	**0.821**
3	**28.39**	28.36	28.11	28.37	28.17	**28.39**
	0.755	0.762	0.736	0.751	0.753	**0.763**
4	26.86	26.75	26.65	26.80	26.72	**26.93**
	0.803	0.803	0.782	0.796	0.801	**0.809**
5	**30.88**	30.75	30.64	30.83	30.65	30.86
	0.812	0.809	0.802	0.805	0.807	**0.814**
6	28.59	28.47	28.49	28.59	28.46	**28.70**
	0.888	0.883	0.882	0.884	0.883	**0.889**
7	30.17	30.18	30.13	30.25	30.22	**30.38**
	0.839	0.840	0.833	0.834	0.843	**0.849**
8	31.58	31.38	31.41	31.52	31.34	**31.62**
	0.900	0.894	0.897	0.894	0.895	**0.902**
9	27.58	27.58	27.58	27.54	27.40	**27.70**
	0.821	0.822	0.804	0.815	0.818	**0.829**
10	**31.23**	31.04	31.98	31.03	30.98	31.15
	0.823	0.818	0.813	0.811	0.815	**0.824**
Avg.	29.42	29.33	29.35	29.37	29.25	**29.48**
	0.833	0.832	0.823	0.827	0.830	**0.838**

	σ = 30					
	BM3D	LSSC	NCSR	WNNM	S-GHP	Ours
1	28.75	28.62	28.58	28.81	28.60	**28.86**
	0.825	0.820	0.820	0.826	0.818	**0.831**
2	26.18	26.14	26.08	26.14	26.07	**26.27**
	0.734	0.734	0.727	0.724	0.734	**0.745**
3	**26.66**	**26.66**	26.39	26.65	26.43	26.63
	0.692	0.696	0.675	0.691	0.688	**0.697**
4	24.79	24.76	24.64	24.81	24.67	**24.96**
	0.715	0.717	0.697	0.712	0.718	**0.734**
5	29.21	29.04	28.91	29.27	28.99	**29.28**
	0.754	0.744	0.742	0.752	0.751	**0.756**
6	26.35	26.33	26.30	26.38	26.26	**26.51**
	0.824	0.825	0.820	0.822	0.820	**0.831**
7	28.35	28.40	28.38	28.50	28.39	**28.59**
	0.771	0.775	0.770	0.770	0.780	**0.786**
8	29.64	29.54	29.52	29.65	29.43	**29.73**
	0.861	0.858	0.860	0.855	0.853	**0.865**
9	25.44	25.48	25.48	25.46	25.31	**25.60**
	0.740	0.748	0.729	0.738	0.744	**0.754**
10	29.53	**30.03**	29.36	29.43	29.15	29.52
	0.763	**0.781**	0.755	0.755	0.754	0.765
Avg.	27.49	27.50	27.36	27.51	27.33	**27.60**
	0.768	0.770	0.760	0.765	0.766	**0.776**

	σ = 40					
	BM3D	LSSC	NCSR	WNNM	S-GHP	Ours
1	27.41	27.32	27.19	27.49	27.22	**27.53**
	0.784	0.781	0.776	0.782	0.781	**0.791**
2	25.02	24.98	24.87	24.98	24.87	**25.13**
	0.668	0.670	0.651	0.654	0.666	**0.680**
3	25.46	**25.47**	25.10	25.46	25.21	**25.47**
	0.647	0.647	0.621	0.645	0.636	**0.650**
4	23.50	23.48	23.26	23.54	23.34	**23.69**
	0.641	0.643	0.604	0.636	0.639	**0.666**
5	28.06	27.90	27.76	28.14	27.88	**28.15**
	0.709	0.696	0.690	0.709	0.704	**0.713**
6	24.97	24.98	24.90	25.01	24.96	**25.15**
	0.765	0.769	0.761	0.761	**0.775**	**0.775**
7	27.18	27.32	27.22	27.35	27.30	**27.43**
	0.721	0.729	0.717	0.717	0.730	**0.736**
8	28.37	28.32	28.24	28.41	28.21	**28.50**
	0.828	0.826	0.827	0.819	0.829	**0.836**
9	24.15	24.19	23.92	24.19	24.05	**24.30**
	0.677	0.687	0.655	0.675	0.684	**0.693**
10	**28.42**	28.24	28.28	28.32	28.15	28.36
	0.721	0.712	0.710	0.712	0.711	**0.723**
Avg.	26.25	26.22	26.07	26.29	26.12	**26.37**
	0.716	0.716	0.701	0.711	0.716	**0.726**

	σ = 50					
	BM3D	LSSC	NCSR	WNNM	S-GHP	Ours
1	26.40	26.33	26.24	26.51	26.00	**26.56**
	0.749	0.747	0.746	0.751	0.746	**0.758**
2	24.21	24.19	24.10	24.22	24.11	**24.32**
	0.615	0.612	0.585	0.608	0.606	**0.627**
3	24.54	**24.58**	24.21	24.50	24.24	24.51
	0.609	0.610	0.585	0.609	0.595	**0.613**
4	22.64	22.60	22.43	22.71	22.38	**22.83**
	0.579	0.581	0.548	0.582	0.568	**0.617**
5	27.23	27.16	27.01	27.36	27.05	**27.38**
	0.678	0.670	0.664	0.679	0.669	**0.683**
6	24.00	24.00	23.97	24.10	23.89	**24.18**
	0.710	0.717	0.713	0.720	0.707	**0.732**
7	26.33	26.50	26.44	26.63	26.46	**26.65**
	0.681	0.695	0.683	0.688	0.687	**0.700**
8	27.44	27.44	27.38	27.57	27.32	**27.64**
	0.798	0.803	0.802	0.799	0.798	**0.807**
9	23.28	23.29	23.04	23.30	23.04	**23.36**
	0.628	0.635	0.609	0.631	0.609	**0.641**
10	27.63	27.46	27.50	27.63	27.50	**27.68**
	0.690	0.681	0.681	0.687	0.681	**0.693**
Avg.	25.37	25.36	25.23	25.45	25.20	**25.51**
	0.674	0.675	0.662	0.675	0.667	**0.687**

	σ = 100					
	BM3D	LSSC	NCSR	WNNM	S-GHP	Ours
1	23.37	23.71	23.66	23.93	23.36	**23.96**
	0.600	0.647	0.652	0.648	0.637	**0.662**
2	22.00	22.05	21.99	22.16	21.86	**22.21**
	0.464	0.463	0.460	0.466	0.469	**0.481**
3	21.69	21.75	21.50	21.87	21.08	**21.89**
	0.492	0.497	0.484	0.501	0.481	**0.503**
4	20.31	20.36	20.23	20.46	20.04	**20.57**
	0.381	0.384	0.367	0.385	0.397	**0.429**
5	24.29	24.49	24.38	24.78	24.17	**24.85**
	0.549	0.553	0.562	0.575	0.549	**0.579**
6	21.52	21.65	21.55	21.86	21.35	**21.87**
	0.530	0.567	0.560	0.566	0.563	**0.571**
7	23.71	24.24	24.20	24.52	24.08	**24.57**
	0.538	0.576	0.584	0.588	0.580	**0.601**
8	24.35	25.00	24.89	25.12	24.53	**25.19**
	0.650	0.728	0.724	0.710	0.703	**0.741**
9	20.94	21.02	20.89	21.15	20.55	**21.16**
	0.481	0.498	0.487	0.498	0.495	**0.500**
10	24.79	24.97	25.00	25.21	24.57	**25.29**
	0.576	0.576	0.600	0.600	0.579	**0.609**
Avg.	22.70	22.92	22.83	23.11	22.56	**23.16**
	0.526	0.549	0.548	0.554	0.545	**0.568**

Table II: Parameter setting used for our method

Noise level (σ)	(, 20)	(20, 40)	(40, 60)	(60,)
λ	0.54	0.56	0.58	0.59
Max. iter. ($T_{\max}$)	8	12	15	20
Patch number (K)	70	90	120	140
Patch size (M)	6×6	7×7	8×8	9×9

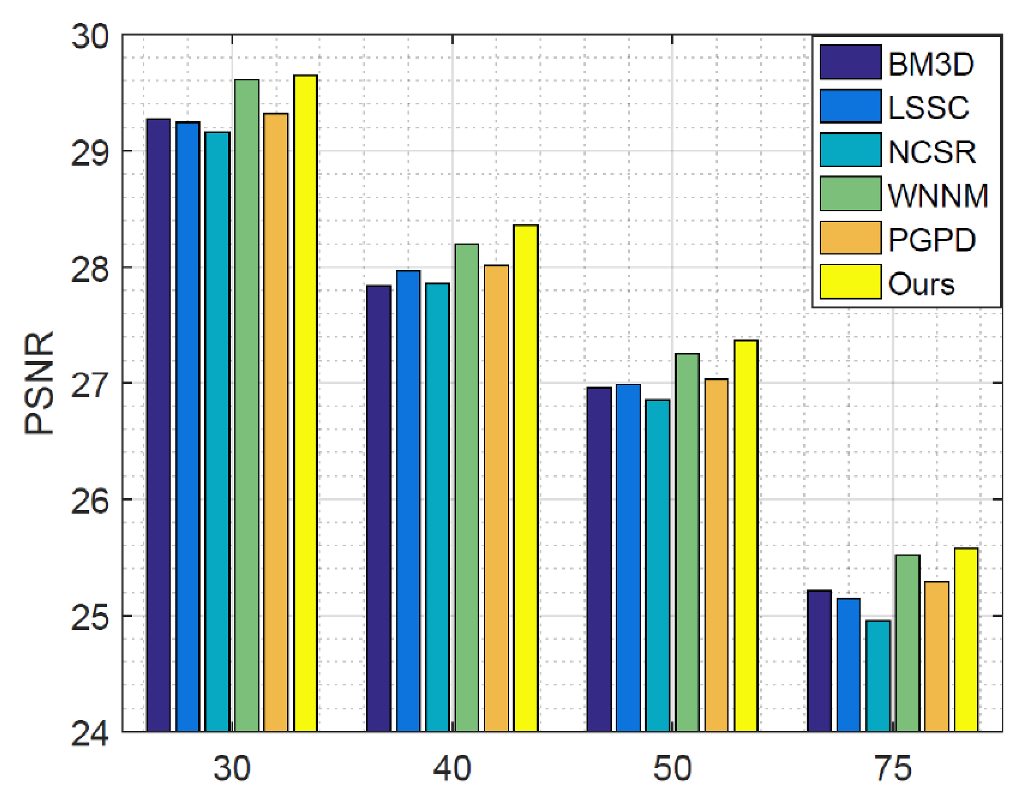

Fig. 1: Mean PSNR obtained by different methods on 11 benchmark images for noise level $\sigma = 30, 40, 50, 75$.

Summary

A new method was proposed for the problem of image denoising. This method integrates the prior based on the wavelet domain global sparsity into an exploited non-local low rank denoising model, allowing it to preserve image details corresponding to fine structures and textures. A new proximal operator of truncated weighted nuclear norm (TWNN) is proposed to recover the high-frequency components of matrices with non-local low-rank patches. This adaptive and flexible operator, which applies less shrinkage to the larger singular values and does thresholding from the ith larger singular value, leads to a higher reconstruction accuracy. An efficient iterative algorithm was also proposed to compute the denoised image, under low rank and wavelet domain sparsity constraints. Experiments showed our method to provide better denoising performance than state-of-the-art approaches.

Reference

[1] Weisheng Dong, Lei Zhang, Guangming Shi, and Xin Li, "Nonlocally centralized sparse representation for image restoration," Image Processing, IEEE Transactions on, vol. 22, no. 4, pp. 1620–1630, 2013.
[2] Mingli Zhang, Christian Desrosiers, and Caiming Zhang, "Effective compressive sensing via reweighted total variation and weighted nuclear norm regularization," in Acoustics, Speech and Signal Processing (ICASSP), 2017 IEEE International Conference on. IEEE, 2017, pp. 1802–1806.
[3]Shuhang Gu, Qi Xie, Deyu Meng, Wangmeng Zuo, Xiangchu Feng, and Lei Zhang, "Weighted nuclear norm minimization and its applications to low level vision," International journal of computer vision, vol. 121, no. 2, pp. 183–208, 2017.